High transverse momentum triggered correlations over a large pseudorapidity acceptance in Au+Au collisions at $\sqrt{s_{NN}}$=200 GeV

B.Alver[4], B.B.Back[1], M.D.Baker[2], M.Ballintijn[4], D.S.Barton[2], R.R.Betts[6], A.A.Bickley[7], R.Bindel[7], W.Busza[4], A.Carroll[2], Z.Chai[2], V.Chetluru[6], M.P.Decowski[4], E.García[6], T.Gburek[3], N.George[2], K.Gulbrandsen[4], C.Halliwell[6], J.Hamblen[8], M.Hauer[2], C.Henderson[4], D.J.Hofman[6], R.S.Hollis[6], R.Hołyński[3], B.Holzman[2], A.Iordanova[6], E.Johnson[8], J.L.Kane[4], N.Khan[8], P.Kulinich[4], C.M.Kuo[5], W.Li[4], W.T.Lin[5], C.Loizides[4], S.Manly[8], A.C.Mignerey[7], R.Nouicer[2,6], A.Olszewski[3], R.Pak[2], C.Reed[4], C.Roland[4], G.Roland[4], J.Sagerer[6], H.Seals[2], I.Sedykh[2], C.E.Smith[6], M.A.Stankiewicz[2], P.Steinberg[2], G.S.F.Stephans[4], A.Sukhanov[2], M.B.Tonjes[7], A.Trzupek[3], C.Vale[4], G.J.van Nieuwenhuizen[4], S.S.Vaurynovich[4], R.Verdier[4], G.I.Veres[4], P.Walters[8], E.Wenger[4], F.L.H.Wolfs[8], B.Wosiek[3], K.Woźniak[3], B.Wysłouch[4]

[1] Argonne National Laboratory, Argonne, IL 60439-4843, USA
[2] Brookhaven National Laboratory, Upton, NY 11973-5000, USA
[3] Institute of Nuclear Physics PAN, Kraków, Poland
[4] Massachusetts Institute of Technology, Cambridge, MA 02139-4307, USA
[5] National Central University, Chung-Li, Taiwan
[6] University of Illinois at Chicago, Chicago, IL 60607-7059, USA
[7] University of Maryland, College Park, MD 20742, USA
[8] University of Rochester, Rochester, NY 14627, USA

(Dated: March 16, 2009)

A measurement of two-particle correlations with a high transverse momentum trigger particle ($p_T^{trig} > 2.5$ GeV/c) is presented for Au+Au collisions at $\sqrt{s_{NN}}$=200 GeV over the uniquely broad longitudinal acceptance of the PHOBOS detector ($-4 < \Delta\eta < 2$). A broadening of the away-side azimuthal correlation compared to elementary collisions is observed at all $\Delta\eta$. As in p+p collisions, the near-side is characterized by a peak of correlated partners at small angle relative to the trigger. However, in central Au+Au collisions an additional correlation extended in $\Delta\eta$ and known as the 'ridge' is found to reach at least $|\Delta\eta| \approx 4$. The ridge yield is largely independent of $\Delta\eta$ over the measured range, and it decreases towards more peripheral collisions. For the chosen p_T^{trig} cut of 2.5 GeV/c, the ridge yield is consistent with zero for events with less than roughly 100 participating nucleons.

PACS numbers: 25.75.-q, 25.75.Bh, 25.75.Gz

One of the most fundamental discoveries at the Relativistic Heavy Ion Collider (RHIC) is that hard-scattered partons seem to interact strongly as they traverse the produced medium [1]. In central Au+Au collisions, the suppression of the single-particle spectra at high p_T relative to binary scaling of p+p [2–4] and the disappearance of back-to-back high p_T pairs [5] are consistent with surface emission of jets due to the presence of an opaque medium that completely absorbs jets directed at the interior.

However, the energy and momentum of the away-side jet must be present in the final state, motivating the study of correlations between high p_T triggers and lower p_T associated particles. Previous such measurements have shown that the absorbed jet energy manifests itself in an away-side structure centered at $\Delta\phi = \pi$ that is broad in $\Delta\phi$ compared to p+p [6, 7] and in an enhanced correlation near $\Delta\phi \approx 0$ observed by the STAR detector to extend at least to $|\Delta\eta| < 1.7$, a phenomenon called the 'ridge' [8]. Although the ridge has been qualitatively described in this narrow $\Delta\eta$ region by a diverse assortment of proposed mechanisms [9–14], the origin of the structure is still not well understood.

The correlated yield of charged hadrons associated with a high transverse momentum trigger particle ($p_T > 2.5$ GeV/c) has been measured in collisions of gold nuclei at $\sqrt{s_{NN}}$=200 GeV by the PHOBOS experiment at RHIC. The data are presented as a function of pseudorapidity ($\Delta\eta$) and azimuthal angle ($\Delta\phi$) relative to the trigger over a range of collision centralities, where the number of participating nucleons (N_{part}) has been determined as in previous papers [1, 2]. This measurement allows a unique examination of the ridge (and its dependence on event centrality) at large relative pseudorapidity up to $|\Delta\eta| \approx 4$, placing a quantitative constraint on the possible interpretations of particle production correlated with high p_T trigger particles.

The PHOBOS detector [15] has two azimuthally opposed spectrometer arms, each covering 0.2 radians, which are used to select charged trigger tracks with $p_T > 2.5$ GeV/c within an acceptance of $0 < \eta^{trig} < 1.5$. Associated particles that escape the beam pipe ($p_T \gtrsim 4$ MeV/c at $\eta = 3$, $p_T \gtrsim 35$ MeV/c at $\eta = 0$) are detected in a single layer of silicon comprising the octagon subdetector ($|\eta| < 3$). The loss of acceptance due to gaps in the octagon array is partly recouped by

using the first layers of the vertex and spectrometer detectors. To account for occupancy effects in the octagon and vertex detectors, each associated hit is weighted by the local occupancy, estimated as in [16] from the fraction of hit pads in the surrounding region.

The construction of the per-trigger correlated yield of charged particles $\frac{1}{N_{trig}}\frac{d^2N_{ch}}{(d\Delta\phi)(d\Delta\eta)}$ is described in any given centrality class by the following expression:

$$B(\Delta\eta)\cdot\left[\frac{s(\Delta\phi,\Delta\eta)}{b(\Delta\phi,\Delta\eta)} - a(\Delta\eta)[1+2V(\Delta\eta)cos(2\Delta\phi)]\right].$$

The raw per-trigger distribution of same-event pairs $s(\Delta\phi,\Delta\eta)$ is divided by the raw mixed-event background distribution $b(\Delta\phi,\Delta\eta)$ to account for random coincidences and acceptance effects. This ratio is calculated in 1 mm bins of vertex position along the beam and averaged over the range $-15 < z < 10$ cm. $B(\Delta\eta)$, which converts the flow-subtracted correlation into a conditional yield, is constructed from the single-particle distribution $(dN/d\eta)$ [17] by convolution with the normalized η distribution of trigger particles.

Because elliptic flow is erased in the mixing of tracks and hits from different events, the remaining $\langle v_2^{trig} v_2^{assoc}\rangle$ modulation carried by $s(\Delta\phi,\Delta\eta)$ must also be subtracted. It is approximated by the product $V(\Delta\eta) = \langle v_2^{trig}\rangle\langle v_2^{assoc}\rangle$ using an event plane method that is sensitive to the RMS of v_2 rather than the mean [18]. As such, this approximation is robust against v_2 fluctuations from initial source eccentricity [19] that could otherwise introduce up to a 10% difference. The flow magnitudes are calculated from a parameterization based on published PHOBOS measurements of v_2 as a function of N_{part}, p_T, and η [20], assuming a factorized form. The v_2 of the trigger track is corrected for occupancy effects in the spectrometer, and the v_2 of associated hits is corrected for secondaries. Both of these effects tend to suppress the magnitude of the observed v_2.

The scale factor $a(\Delta\eta)$ is introduced to account for the small difference in multiplicity between signal and mixed-event distributions. Its value – within a few percent of unity in all cases considered – is extracted separately in bins of centrality and $\Delta\eta$, using an implementation of the zero yield at minimum (ZYAM) method [21] that fits the minimum of $\frac{s(\Delta\phi)/b(\Delta\phi)}{1+2Vcos(2\Delta\phi)}$ with a second-order polynomial in the region $0.5 < \Delta\phi < 1.5$ radians. The $\Delta\eta$ dependence of the ZYAM factor is parameterized by the sum of a constant and a Gaussian term. The magnitude and centrality dependence of the constant term are consistent with the bias of the p_T-triggered signal distribution to higher multiplicity that is expected from the known centrality bin widths. The Gaussian term reveals the presence of a long-range $\Delta\eta$ correlation structure underneath the v_2-subtracted $\Delta\phi$ correlations. Its width is consistent with inclusive two-particle correlation measurements [22], as is the centrality dependence of its amplitude after accounting for the dominant $1/N$-dependence due to a trivial dilution from uncorrelated particles. The uncertainty on the value of $a(\Delta\eta)$ is estimated from the error matrix of a 2-D fit to the extracted ZYAM parameters in N_{part} and $\Delta\eta$. The subtraction of elliptic flow from the raw correlation using this implementation of the ZYAM method is illustrated in Fig. 1, where the shaded band represents the flow uncertainty and the dashed line the extracted ZYAM scale factor, $a(\Delta\eta)$.

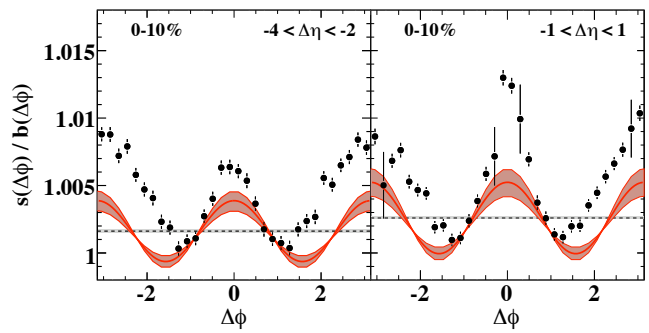

FIG. 1: (color online) Ratio of signal to background for the 10% most central collisions at long-range (left) and short-range (right). The estimated flow modulation (scaled by $a(\Delta\eta)$) and its uncertainty are represented by the solid line and shaded band. The uncertainty on the ZYAM parameter is represented by the narrow band around the dashed line.

The dominant systematic error in this analysis comes from the uncertainty in estimating the magnitude of $\langle v_2^{trig}\rangle\langle v_2^{assoc}\rangle$. This flow uncertainty is typically on the order of 15-20%. It reaches 50% in the most central 3% of collisions, although here $V(\Delta\eta)$ is quite small (≤ 0.0008) compared to the resulting jet correlation.

To understand the effects of the hot, dense medium on correlated particle production, the PHOBOS Au+Au data is compared to p+p events simulated with PYTHIA [23]. The prominent features of the p+p correlation, shown in Fig. 2(a), are a jet-fragmentation peak centered at $\Delta\phi = \Delta\eta = 0$ and an away-side structure centered at $\Delta\phi = \pi$ that is similarly narrow in $\Delta\phi$ but extended in $\Delta\eta$, since the hard scattering can involve partons with very different fractions of the proton momentum.

In central Au+Au collisions, particle production correlated with a high p_T trigger is strongly modified as shown in Fig. 2(b). Not only is the enhanced away-side yield much broader in $\Delta\phi$, the near-side peak at $\Delta\phi \approx 0$ now sits atop a pronounced ridge of correlated partners extending continuously and undiminished all the way to $\Delta\eta = 4$.

To examine the near-side structure more closely, the correlated yield is integrated over the region $|\Delta\phi| < 1$ and plotted as a function of $\Delta\eta$ in Fig. 2(c). For the most

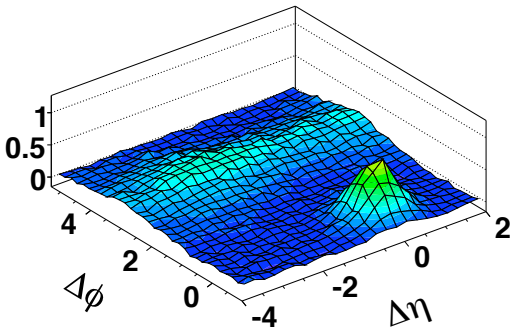

(a) p+p PYTHIA

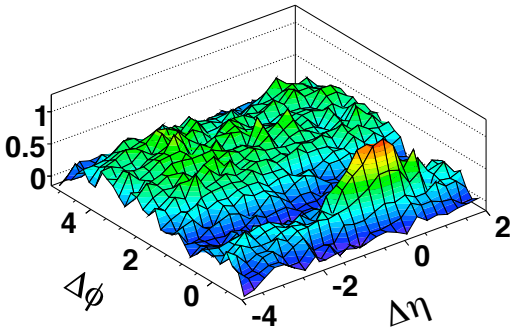

(b) Au+Au 0-30% (PHOBOS)

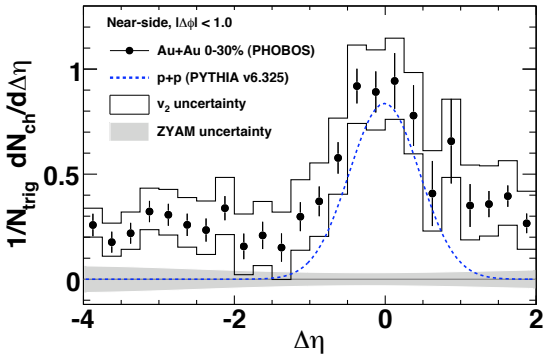

(c) Near-side $\Delta\eta$ projection ($|\Delta\phi| < 1$)

FIG. 2: (color online) Per-trigger correlated yield with $p_T^{trig} > 2.5$ GeV/c as a function of $\Delta\eta$ and $\Delta\phi$ for $\sqrt{s}$ and $\sqrt{s_{NN}}$=200 GeV (a) PYTHIA p+p and (b) PHOBOS 0-30% central Au+Au collisions. (c) Near-side yield integrated over $|\Delta\phi| < 1$ for 0-30% Au+Au compared to PYTHIA p+p (dashed line) as a function of $\Delta\eta$. Black boxes represent the uncertainty from flow subtraction. The error on the ZYAM procedure is shown as a gray band at zero. All systematic uncertainties are 90% confidence level.

central 30% of Au+Au collisions, there is a significant and relatively flat correlated yield of about 0.25 particles per unit pseudorapidity far from the trigger.

A more detailed examination of the correlation structure is possible by projecting the correlation onto the $\Delta\phi$ axis as in Fig. 3. In the top row of that figure, the correlated yield in Au+Au is compared for five centrality bins (40-50%, 30-40%, 20-30%, 10-20% and 0-10%) to PYTHIA-simulated p+p events at short-range (i.e. integrated over the region $|\Delta\eta| < 1$). In the bottom row, the same comparison is shown at long-range (i.e. integrated over the region $-4 < \Delta\eta < -2$).

Focusing first on the away-side correlation, a number of features become apparent. First, the shape of the correlation is considerably broader in $\Delta\phi$ for Au+Au collisions compared to p+p in all measured centrality bins. Additionally, the magnitude of the away-side yield is enhanced relative to p+p, increasingly so for more central Au+Au collisions. Finally, the away-side correlation seems to have a very similar shape and centrality dependence at both short- and long-range. This last observation is explored more quantitatively in Fig. 4, where integrated away-side yields ($\Delta\phi > 1$) are presented as a function of participating nucleons at short- and long-range (open and filled squares respectively).

The near-side region also shows a strong modification spanning the full measured pseudorapidity range. At short-range (top row of Fig. 3), a narrow peak at $\Delta\phi \approx 0$ is observed. In central collisions, this peak has a large contribution in excess of the p+p jet yield. The near-side, short-range correlation decreases in magnitude with decreasing centrality, reaching the same height as p+p in the 40-50% bin.

At long-range (bottom row of Fig. 3), the persistence of the ridge correlation to very large $\Delta\eta$ is evident in the peak at $\Delta\phi \approx 0$ for central Au+Au collisions. This effect is completely absent in more elementary systems. The ridge yield also decreases in magnitude for more peripheral collisions until it disappears in the 40-50% bin.

The similar centrality dependence of the short- and long-range yields in excess of the p+p jet correlation suggests a decomposition of the near-side correlation into distinct jet and ridge components. Such a separation is supported by previous STAR measurements of the associated particle p_T spectra, the centrality independence of the jet-like yield, and the ridge-subtracted fragmentation function [8].

In Fig. 4, the integrated ridge yield at long-range (filled circles) is compared to the short-range yield (open circles) after subtraction of a jet component corresponding to the PYTHIA yield. A more precise agreement between these two yields might be achieved for an approximately 15% smaller jet component, inducing all the open circles to move up by 0.07. Nonetheless, already for this simple assumption, the ridge yield is shown to be the same within experimental uncertainties at all $\Delta\eta$. It decreases as one goes towards more peripheral collisions and is consistent with zero in the most peripheral bin analyzed (40-50%). While the systematic errors do not completely exclude a smooth disappearance of the ridge as one approaches p+p collisions, these data suggest that with a 2.5 GeV/c trigger particle the ridge may already have disappeared

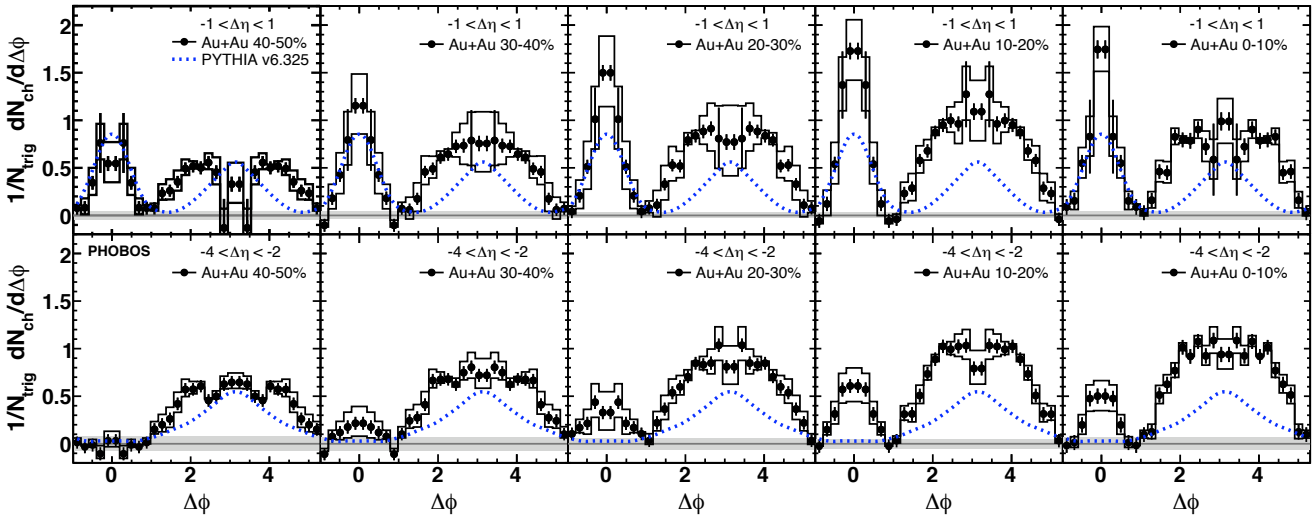

FIG. 3: (color online) Projections of the correlated yield versus $\Delta\phi$ at short-range (top row, $-1 < \Delta\eta < 1$) and long-range (bottom row, $-4 < \Delta\eta < -2$) for five centrality bins (most central on right). Points have been reflected about $\Delta\phi = 0$ and averaged. The dashed line is p+p PYTHIA for comparison. 90% C.L. systematic uncertainties are presented as in Fig 2c.

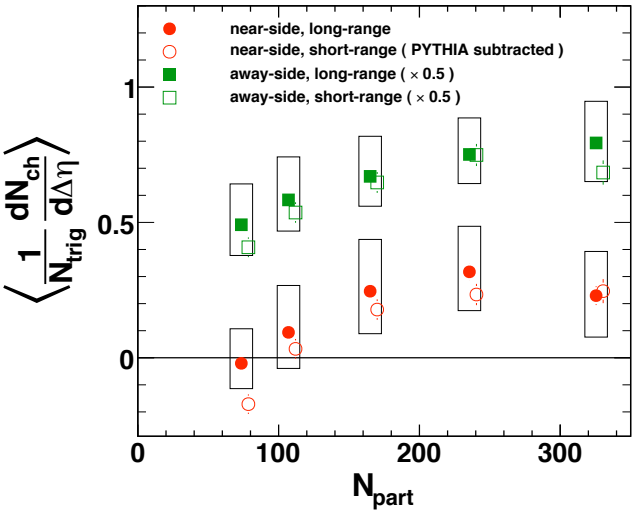

FIG. 4: (color online) Average near-side ($|\Delta\phi| < 1$) and away-side ($\Delta\phi > 1$) yields as a function of N_{part} at both short-range ($|\Delta\eta| < 1$) and long-range ($-4 < \Delta\eta < -2$). The near-side yield at short-range has the full PYTHIA jet yield subtracted from it. For clarity of presentation, the open points have been offset slightly and the away-side yields scaled down by a factor of 2. Boxes correspond to the combined 90% systematic uncertainties on the v_2 estimate and ZYAM procedure.

by $N_{part} = 80$ (about 45% central).

In this letter, PHOBOS measurements of the ridge at small $\Delta\phi$ have been presented over a broad range of $\Delta\eta$. The fact that in central collisions the ridge extends to at least four units of pseudorapidity away from the trigger is a powerful constraint on theories that strive to explain the nature of particle production in heavy ion collisions. More quantitative theoretical studies will be required to determine which proposed mechanisms can consistently describe the broad extent of the ridge and its dependence on collision geometry.

This work was partially supported by U.S. DOE grants DE-AC02-98CH10886, DE-FG02-93ER40802, DE-FG02-94ER40818, DE-FG02-94ER40865, DE-FG02-99ER41099, and DE-AC02-06CH11357, by U.S. NSF grants 9603486, 0072204, and 0245011, by Polish MNiSW grant N N202 282234 (2008-2010), by NSC of Taiwan Contract NSC 89-2112-M-008-024, and by Hungarian OTKA grant (F 049823).

[1] B. B. Back et al., Nucl. Phys. **A757**, 28 (2005).
[2] B. Alver et al., Phys. Rev. Lett. **96**, 212301 (2006).
[3] S. S. Adler et al., Phys. Rev. **C69**, 034910 (2004).
[4] J. Adams et al., Phys. Rev. Lett. **91**, 172302 (2003).
[5] C. Adler et al., Phys. Rev. Lett. **90**, 082302 (2003).
[6] A. Adare et al., Phys. Rev. **C77**, 011901 (2008).
[7] J. Adams et al., Phys. Rev. Lett. **95**, 152301 (2005).
[8] J. Putschke, J. Phys. **G34**, S679 (2007).
[9] N. Armesto, C. A. Salgado, and U. A. Wiedemann, Phys. Rev. Lett. **93**, 242301 (2004).
[10] C. B. Chiu and R. C. Hwa, Phys. Rev. **C72**, 034903 (2005).
[11] E. V. Shuryak, Phys. Rev. **C76**, 047901 (2007).
[12] V. S. Pantuev (2007), arXiv:0710.1882.
[13] C.-Y. Wong (2007), arXiv:0712.3282.
[14] S. Gavin, L. McLerran, and G. Moschelli (2008), arXiv:0806.4718.
[15] B. B. Back et al., Nucl. Instrum. Meth. **A499**, 603 (2003).
[16] B. B. Back et al., Physical Review Letters **94**, 122303 (2005).
[17] B. B. Back et al., Phys. Rev. Lett. **91**, 052303 (2003).
[18] B. Alver et al., Phys. Rev. **C77**, 014906 (2008).
[19] B. Alver et al. (2007), nucl-ex/0702036.

[20] B. B. Back et al., Phys. Rev. **C72**, 051901 (2005).
[21] N. N. Ajitanand et al., Phys. Rev. **C72**, 011902 (2005).
[22] B. Alver et al. (2008), arXiv:0812.1172.
[23] T. Sjöstrand et al., Comput. Phys. Commun. **135**, 238 (2001).